Defect incorporation in In-containing layers and quantum wells: experimental analysis via deep level profiling and optical spectroscopy

F. Piva[1*], C. De Santi[1], A. Caria[1], C. Haller[2], J.-F. Carlin[2], M. Mosca[2,3], G. Meneghesso[1], E. Zanoni[1], N. Grandjean[2], M. Meneghini[1]

[1] *Department of Information Engineering, University of Padova, Italy*

[2] *Institute of Physics, Ecole Polytechnique Fédérale de Lausanne (EPFL), Switzerland*

[3] *Department of Engineering, University of Palermo, I-90128, Palermo, Italy.*

Abstract

Recent studies demonstrated that the performance of InGaN/GaN quantum well (QW) light emitting diodes (LEDs) can be significantly improved through the insertion of an InGaN underlayer (UL). The current working hypothesis is that the presence of the UL reduces the density of non-radiative recombination centers (NRCs) in the QW itself: during the growth of the UL, surface defects are effectively buried in the UL, without propagating towards the QW region. Despite the importance of this hypothesis, **the concentration profile of defects in the quantum wells of LEDs with and without the UL was never investigated in detail**. This paper uses combined capacitance-voltage (C-V) and steady-state photocapacitance (SSPC) measurements to experimentally identify the defects acting as NRCs and to extract a depth-profile of the traps, thus proving the incorporation upon indium-reaction. Specifically: (i) we demonstrate that LEDs without UL have a high density ($9.2x10^{15}$ cm^{-3}) of defects, compared to samples with UL ($0.8x10^{15}$ cm^{-3}); (ii) defects are located near midgap (E_C-1.8 eV, corresponding to E_i-E_T~0.3eV), thus acting as efficient NRCs; (iii) crucially, the density of defects has a peak within the QWs, indicating that traps are segregated at the first grown InGaN layers; (iv) we propose a model to calculate trap distribution in the QW, and we demonstrate a good correspondence with experimental data. These results provide unambiguous demonstration of the role of UL in limiting the propagation of defects towards the QWs, and the first experimental characterization of the properties of the related traps.

Introduction

Light-emitting diodes (LEDs) with InGaN/GaN quantum well (QW) are efficient structures for electroluminescence in the near-UV and blue spectral region, with internal quantum efficiency (IQE) that reach values over 80% [1]. The use of an InGaN underlayer (UL) below the QW region has been proposed as an effective solution to increase the efficiency of the LEDs. By increasing the concentration of indium inside the UL, the number of defects incorporated in the subsequent QW growth decreases [2]. These results are consistent also with reports by other groups [3]–[14], where the performance of GaN *p-i-n* diodes was improved via a similar approach. In addition to the concentration of indium, also the growth temperature can have a role in the reduction of the defects [15].

Several mechanisms have been proposed to explain the improved performance obtained through the use of the UL: a) the UL acts as a reservoir of electrons, that improves the injection efficiency [16]; b) the UL improves the crystalline quality, reducing the density of dislocations in the QWs [17]; c) the UL reduces the strain in the QW region, thus minimizing the quantum confined Stark effect (QCSE) [18]. Recently, a study on single QW samples has shown that the purpose of InGaN UL is to increase the IQE of InGaN QWs by reducing the non-radiative center density in the QWs, [1] as originally proposed by Armstrong *et al*. [19].

Despite the importance of this hypothesis, experimental profiling of the defects near the active region (with consequent evidence of the fact that the UL effectively reduces the density of defects) has not been reported to date in the literature. Several different techniques have been used to this aim: a) secondary ion mass spectroscopy (SIMS) proved to be ineffective [2], since it can track only specific impurities (like O, C, Mg, Fe, and Ca), with a relative low sensitivity (10^{16} cm^{-3} in most cases); b) capacitance-voltage (C-V) analysis [19], [20] can detect changes in free charge density, without describing the properties of the related defects; c) non-radiative defects are supposed to be located near midgap where, according to the Shockley-Read-Hall theory, they have maximum recombination probability [21]. However deep-level transient spectroscopy and admittance spectroscopy [22] are not sensitive to mid-gap defects in GaN (typically these techniques detect levels located at a maximum of 1 eV below the conduction band energy); d) recent reports [19], [20], [22] suggested the existence of midgap-defects through optical spectroscopy, without investigating the difference in concentration in the QW region for samples with and without UL.

The aim of this paper is to bridge this gap, by providing an experimental proof of the reduction in point defects obtained through the use of an UL. To advance the understanding, (i) we unambiguously demonstrate that the use of an UL can reduce the density of defects in the QW region; (ii) we show that defects are located near midgap (at E_C-1.8 eV for a QW emission energy of 3.1 eV, corresponding to E_i-E_T~0.3eV), thus acting as effective NRCs; (iii) thanks to the use of a specific test structure, with heavily doped n-type barriers surrounding the QWs, we are able to obtain a profile of defect concentration in the QWs; (iv) we demonstrate that for the sample without UL defect concentration peaks within the QW, thus experimentally proving that the first InGaN layers grown capture most of the surface defects, thus impeding a further propagation towards the p-side; (v) we propose a model to calculate the defect density and profile in the QW region, and demonstrate a good agreement with experimental data. These results were obtained thanks to combined capacitance-voltage and steady-state photocapacitance measurements, on the test structures described below.

Experimental results

For this analysis we used two comparable wafers, whose only difference is the presence or absence of a nearly lattice-matched InAlN UL below the QW (Figure 1). The InAlN UL has been shown to act similarly to an InGaN UL [4] as In is the key ingredient to trap the defects. The analyzed LEDs have a sapphire substrate, a GaN buffer, followed by either an InAlN UL (2 layers GaN 1.75 nm/$In_{0.17}Al_{0.83}N$ 2.1 nm both doped $1.5x10^{20}$, 22 layers superlattice constituted of GaN 1.75 nm/$In_{0.17}Al_{0.83}N$ 2.1 nm both doped $3x10^{18}$) with a thin GaN buffer (sample labeled as w/ UL), or only by a thin GaN buffer (sample labeled as w/o UL). Above this layer, the InGaN single QW layer was grown. The QW was sandwiched between two highly-doped (10^{18} cm^{-3}) n-type barriers.

These barriers are necessary to make sure that at zero bias the depleted region does not include the QW, thus permitting an efficient defect analysis of the QWs via capacitance and SSPC measurements. Finally, the electron blocking layer (EBL) and the p-type GaN cap were grown.

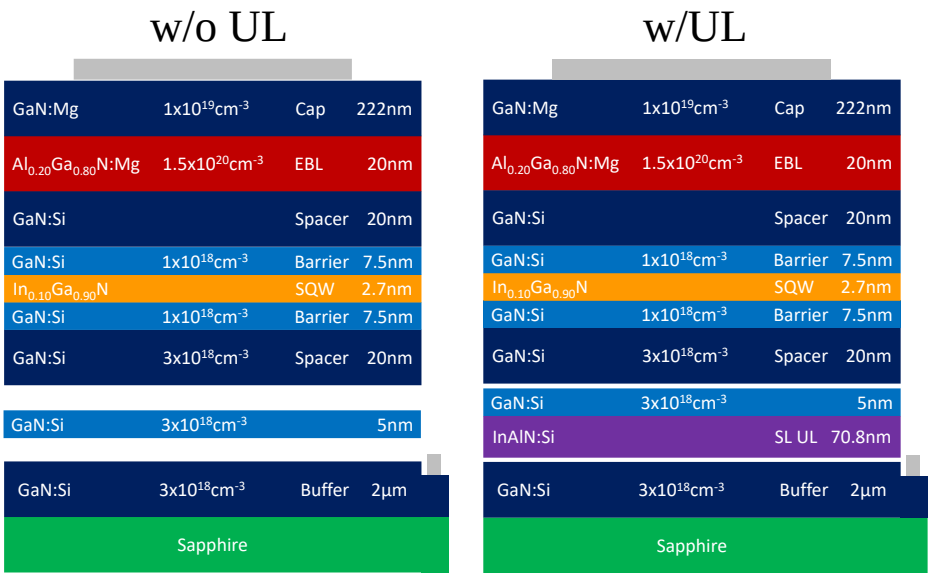

Figure 1 - Internal structure of the LEDs. On the left the one without superlattice underlayer, on the right the one with superlattice underlayer

To compare the two wafers, EQE characterization (between $2x10^{-3}$ A/cm^2 and 600 A/cm^2) and current-voltage (I-V) measurements were carried out. To detect deep (midgap) defects, we carried out steady-state photocapacitance (SSPC) measurements, performed by illuminating the samples with monochromatic radiation with energy ranging from 1.1 eV to 3.65 eV, with bias of 0V. Additional measurements were carried out at fixed photon energy (1.95 eV, to deplete midgap defects), with different voltages from -2.5 V to 2 V with step of 50 mV, to obtain a concentration profile of the deep levels. Finally, light-assisted C-V measurements were carried out, with a photon energy of 1.95 eV. These measurements, both in dark and in light conditions, were done with a small signal of 50 mV and voltage steps of 50 mV, at two different frequencies of 1 kHz and 1 MHz, in order to estimate correctly both the depletion width and the density of free charge.

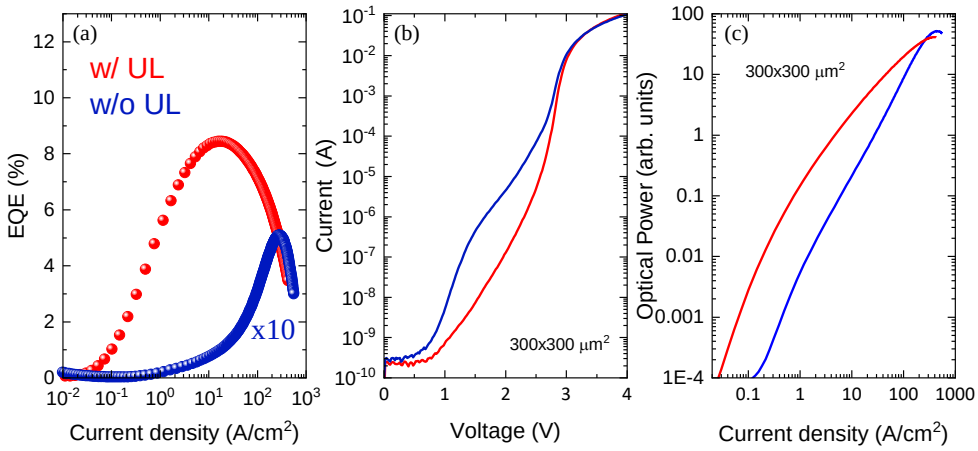

Figure 2 – (a) Relative EQE versus current density, (b) current – voltage characteristic of representative samples with and without underlayer, (c) optical power versus current density.

Figure 2 reports the electro-optical characteristics of the two wafers. Specifically, the EQE (Figure 2(a)) measurements indicate that the sample with UL has a higher efficiency, consistently with previous studies on the topic [2], [4]. The I-V characteristics (Figure 2(b)) indicates that the sample without UL has a much higher current below the turn on voltage (between 1 V and 2.5 V). Sub-turn on leakage is typically ascribed to midgap defects [23], [24]; results in Figure 1 (b) give therefore a first indication that the samples with and without UL differ in the density of midgap defects.

To characterize the presence of defects, SSPC measurements were carried out in the range between 1.1 eV and 3.65 eV. The measurement setup is composed by a Xenon Arc lamp with a wide emission spectrum, in order to cover all the photon energy range of interest, a monochromator to extract a single and accurate wavelength, a filter wheel to remove second harmonic effects, and a lens to focus the light inside an optical fiber used to bring light to the sample. The capacitance measurement is done by a LCR meter properly synchronized with the rest of the setup. After setting the bias (0 V), we maintained the sample in dark conditions for 20 seconds, in order to reach a constant value of the capacitance. After that, we exposed the LEDs to monochromatic light for 20 seconds, to empty all the traps (this results in an exponential capacitance increase, Figure 3(a)). At the end, we brought back the sample to dark conditions for 200 seconds, restore the dark capacitance level. As shown in Figure 3(a), no significant signal was detected for low photon energies (<1.6 eV). A significant capacitance variation was obtained for photon energies higher than 1.6 eV, as will be discussed in the following. Remarkably, we found that the wafer with UL has a much lower SSPC signal (Figure 3(b)), that is ascribed to a lower defect concentration.

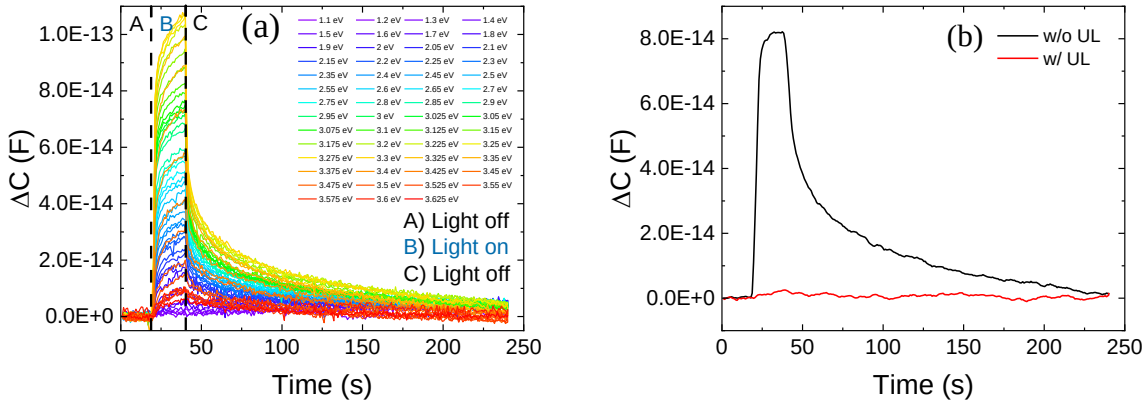

Figure 3 - (a) SSPC capacitance transients measured by illuminating the sample with monochromatic light at different photon energies, (b) comparison between transients measured on samples without and with underlayer with monochromatic excitation at 2.5 eV (bias=0 V). It is worth noticing that the transient of the sample w/ UL is more than an order of a magnitude lower than the other one.

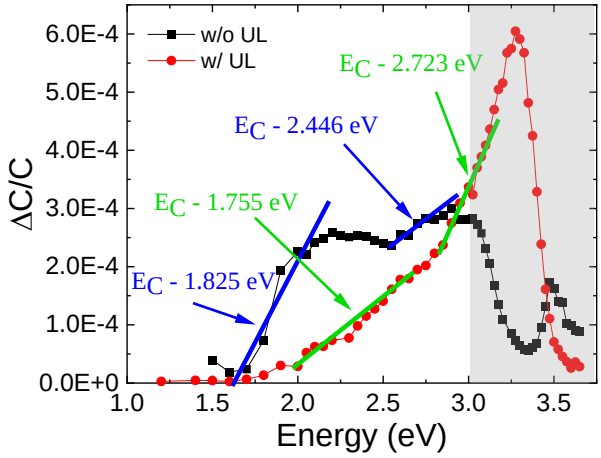

Figure 4 - Comparison between steady state photo-capacitance measurements. The ionization energy level are extracted from PCS fitted with Pässler model [25] as in [19]. Straight lines are guides to the eye, to help the reader understanding the onset in SSPC related to each trap

Figure 4 reports the steady state photo-capacitance spectra of the two wafers. Both samples reveal the presence of near mid-gap defects with ionization energy of about E_C – 1.8 eV (corresponding to E_i-E_T~0.3 eV for the 3.1 eV bandgap under consideration), whose concentration is much higher in the sample w/o UL (the amplitude of the SSPC signal gives a quantitative estimate of the density of defects responding at each wavelength). The samples present another defect level each, at about E_C – 2.5 eV for the sample w/o UL and E_C – 2.7 eV for the sample w/ UL. The optical activation energies of these levels were extracted from the spectral dependence of optical cross-section (PCS) fitted by the model proposed by *Pässler* [25] (fitting not reported for brevity). It is worth noticing that the inflexion above 3.0 eV is related to generation in the QW. Beyond 3 eV (shaded region in

Figure 3), the SSPC measurements do not provide reliable data on defects; for this reason, the corresponding data are shaded in Figure 3.

The onset found in both devices around 1.8 eV is relevant, in terms of SRH recombination, since it represents a near mid-gap defect. For this reason, we decided to do an additional investigation in order to extract the profile of defect concentration in the material. We performed C-V capacitance measurement to derive the apparent charge profile. Then we correlated, for each voltage, the ΔC/C signal measured by SSPC measurements with the related density of defects, through the well known formula $N_T = 2\,\frac{\Delta C}{C}\,N$, where N_T is the trap concentration and N is the density of free charge at a given voltage.

From this measurement, we were able to extract the approximate profile of the traps in the structure (Figure 5(b)).

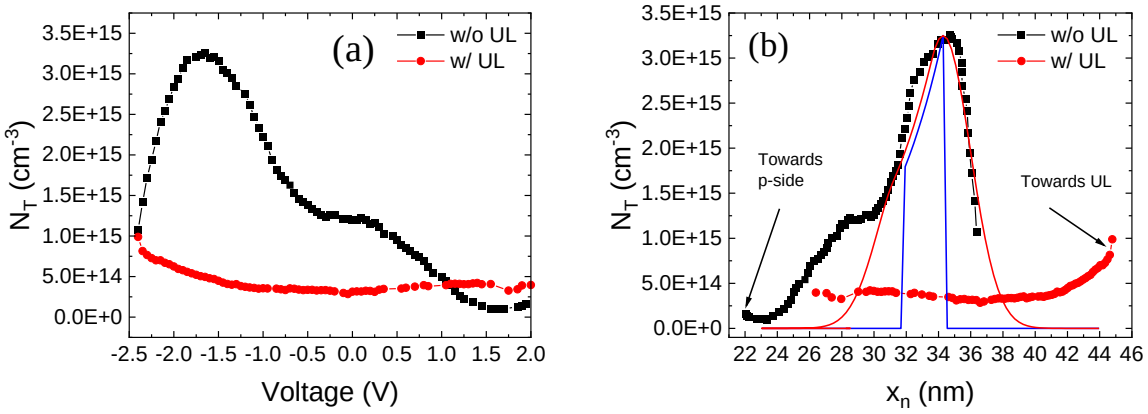

Figure 5 – Concentration of the traps in the structure as a function of (a) applied voltage and (b) distance from the junction. The blue line is the model of the NRCs incorporation in the QW. The red line is the convolution of the model with a Gaussians which has a width of 5 nm. Note that the concentration values estimated by SSPC are slightly underestimated than the real ones (extrapolated with higher accuracy by light C-V measurements, see below) due to the intrinsic resolution/sensitivity limit of SSPC. To convert (a) into (b), we simply calculated the width of the space charge region (with the approximation of a p^{++}/n junction) from the C-V measurement, and plotted the concentration of traps as a function of it in (b).

Differently from previous papers [26], we were able to estimate the profile of the trap density *in the QWs* for samples with and without underlayer. Figure 5 demonstrates a measurable peak of trap concentration near/below the QW for the sample w/o UL (peak around 34 nm in Figure 5(b)). The density of defects then decreases moving towards the p-side, falling below 10^{14} cm^{-3}. On the other hand, the sample w/ UL presents a constant concentration (about $0.5x10^{15}$ cm^{-3}) of defects in the QW region and a slightly increment on the right-hand side, toward the UL (not reached by the SSPC measurements). This indicates that the UL can effectively incorporate defects during growth, thus impeding the propagation towards the QW region.
It has been shown that defects present at the surface of GaN after the high temperature (HT) buffer react with In atoms during the growth of In containing alloys and then get incorporated in the layer to form point defects (PDs) that are efficient NRCs [2]. This incorporation process was modeled

considering a surface segregation phenomenon [27], [28], where the concentration of PDs, in the i^{th} monolayer ML, is given by $[\mathrm{PD}]_i = \theta_i R / e_{\mathrm{ML}} = \theta_i (R_{\mathrm{GaN}} - x_{\mathrm{In},i} p) / e_{\mathrm{ML}}$ with θ_i the surface defect (SD) density, R_{GaN} the segregation coefficient of SDs in GaN (0.9991), p the interaction coefficient between indium and SDs (0.7), e_{ML} the thickness of the ML, and x_{In} the indium concentration. The values of R_{GaN} and p are coming from Ref. [28]. Thus, after each ML, the SD density is given by $\theta_i = \theta_{i-1} - \theta_{i-1}(R_{\mathrm{GaN}} - x_{\mathrm{In},i} p)$. From this model, it is clear that the PD concentration in the QW gradually decreases in each ML. For both samples, the initial SD density (θ_0) is the same as they are generated during the high-temperature growth of the GaN buffer [28], [29]. When an InAlN/GaN SL is introduced, SDs strongly incorporate since the indium content is high (17%), see Figure 6(a). For the sample without UL, the incorporation of SD in the GaN spacer is negligible, even at low-temperature. As a consequence, the SD density before the growth of the QW is very high, similar to that at the end of the HT GaN buffer, resulting in a high concentration of PDs in the QW after their reaction with In atoms. In this case, the PD density calculated by the model is 4×10^{15} cm^{-2}, which is orders of magnitude higher than the value obtained with an InAlN/GaN SL (7×10^{4} cm^{-2}). A difference can be seen between the experimental data (Figure 5(b)) and the model. Indeed, the probed area during the measurement is large (300×300 μm^2), which may explain the broadening over few nm due to depth fluctuations. We then convolute the model with a Gaussian of 5 nm to account for the experimental broadening. Our model qualitatively reproduces the first part of the defect incorporation in the QW. The presence of traps in the top barrier (x_n < 30 nm) could be due to the surface segregation of In atoms in the GaN barrier, which is not taken into account in the model.

As a final step of this analysis, we applied the method proposed by Armstrong et al. [26] to determine the net value of concentration of traps in the various regions, with high accuracy. We started by doing C-V measurements in the dark and under monochromatic illumination (1.95 eV), to study the effects of only the near midgap-states (1.825 eV), without contributions from the other levels (that would require higher-energy excitation). After that, we evaluated the difference ΔV between the voltage values at the same capacitance in the two conditions of illumination (Figure 7(a)). So, we defined two regions for each sample, QW and over QW for sample w/o UL, and QW and under QW for sample w/ UL. By solving the equation:

$$\Delta V = \frac{q}{\varepsilon} \int_0^{x_d} x\, n_t(x)\, dx = \frac{q}{\varepsilon} N_T \int_0^{x_d} x\, dx$$

we were able to find the concentration of traps in the different regions, as reported in Figure 7(b).

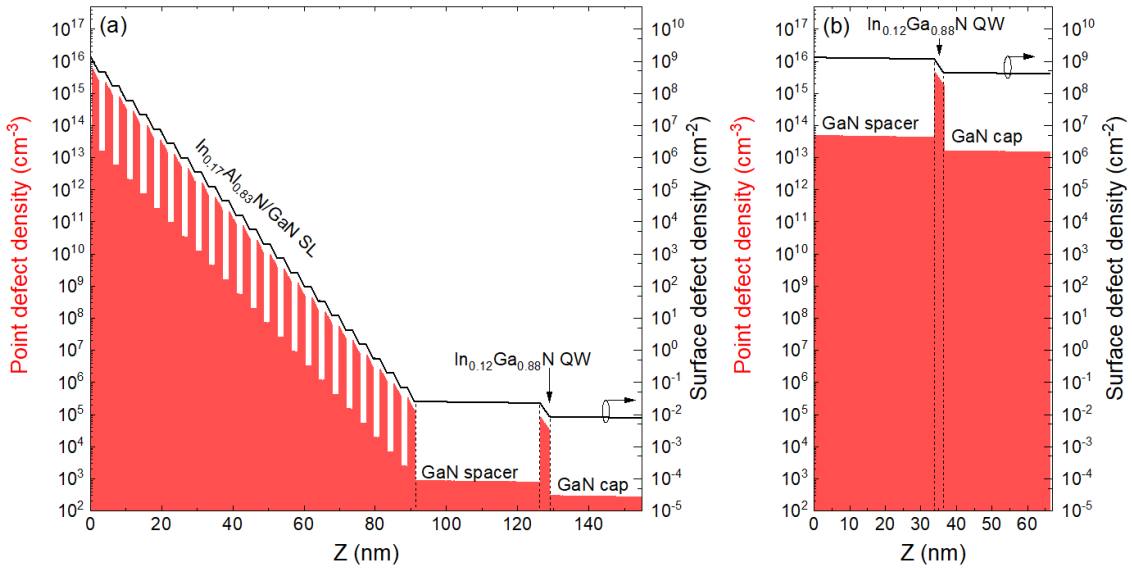

Figure 6 - Point defect concentration in the layers (*red*) and density of surface defects during the growth (*grey*) with UL (a) and w/o UL (b). The x-axis scale is the sample thickness with z=0 at the end of the high-temperature GaN buffer. We use a concentration θ_0 equal to 1.3×10^9 cm^{-2}

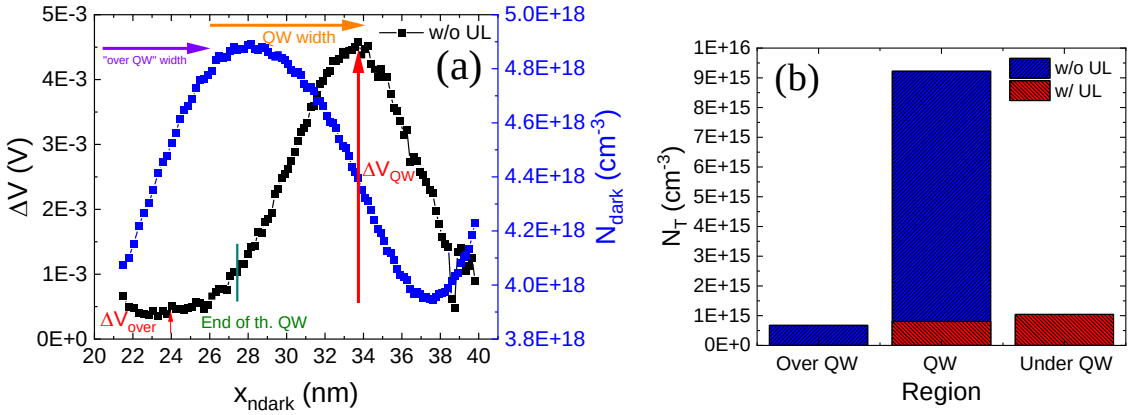

Figure 7 - (a) Left axis: profile of the difference between the voltages at the same capacitance measured under dark condition and under monochromatic illumination for the sample w/o UL. Right axis: apparent charge profile in dark condition calculated by C-V measurement used to establish the position of the QW. The arrows indicate the exact initial and final values of each physical region and the voltages used in the calculation. (b) Net trap concentration for the two samples. It is worth noticing that the only region where N_T can be compared for the two wafers is the QW region (which is the region of interest). In fact, due to the adopted voltage ranges (selected in order to avoid device breakdown and/or turn-on) and to the differences in device capacitance, the region above the QW could be probed only in the sample without underlayer, while the region below the QW could be probed only in the sample with underlayer. To the authors' opinion, this is not a limitation, since our interest is to explore the density of defects in the active region, that can be effectively probed in both wafers.

As can be seen from Figure 7(b), the concentration of defects in the QW region for the sample w/o UL ($9.2x10^{15}$ cm^{-3}) is nearly ten times higher than the sample w/ UL ($0.8x10^{15}$ cm^{-3}). This is a clear indication about the effectiveness of the UL in blocking the propagation of defects towards the QWs; these results are also well correlated with the results of I-V and EQE-J characterization, where we ascribed the worse performance of sample w/o UL to the higher defects density.

Conclusions

In conclusion, we presented experimental demonstration that the insertion of the UL in InGaN LEDs can significantly reduce the density of defects in the QW region, and presented information on the properties of the related traps and their profile. From the results of this analysis, we conclude that the InGaN UL blocks further propagation of the defects toward the active region, providing a constant concentration of traps in the explored region; with UL, the density of point defects is an order of magnitude lower than w/o UL. We also proposed a model to account for defect incorporation within the QW and demonstrated a good agreement with the experimental results obtained by optical spectroscopy. Finally, we demonstrated that the defects are mid-gap (E_C-1.8 eV for 3.1 eV bandgap) and they act as effective NRCs, causing thereby an important decrease in the LED performance.

References

Data available on request from the authors. The data that support the findings of this study are available from the corresponding author upon reasonable request.

[1] A. David, N. G. Young, C. Lund, and M. D. Craven, "Review—The Physics of Recombinations in III-Nitride Emitters," *ECS J. Solid State Sci. Technol.*, vol. 9, no. 1, p. 016021, 2020, doi: 10.1149/2.0372001jss.

[2] C. Haller, J. F. Carlin, G. Jacopin, D. Martin, R. Butté, and N. Grandjean, "Burying non-radiative defects in InGaN underlayer to increase InGaN/GaN quantum well efficiency," *Appl. Phys. Lett.*, vol. 111, no. 26, Dec. 2017, doi: 10.1063/1.5007616.

[3] S. R. Alugubelli *et al.*, "Determination of electronic band structure by electron holography of etched-and-regrown interfaces in GaN p-i-n diodes," *Appl. Phys. Lett.*, vol. 115, no. 20, Nov. 2019, doi: 10.1063/1.5127014.

[4] C. Haller, J. F. Carlin, M. Mosca, M. D. Rossell, R. Erni, and N. Grandjean, "InAlN underlayer for near ultraviolet InGaN based light emitting diodes," *Appl. Phys. Express*, vol. 12, no. 3, Mar. 2019, doi: 10.7567/1882-0786/ab0147.

[5] J.-Y. Park, J.-H. Lee, S. Jung, and T. Ji, "InGaN/GaN-based green-light-emitting diodes with an inserted InGaN/GaN-graded superlattice layer," *Phys. status solidi*, vol. 213, no. 6, pp. 1610–1614, Jun. 2016, doi: 10.1002/pssa.201533092.

[6] Y. Xia, W. Hou, L. Zhao, M. Zhu, T. Detchprohm, and C. Wetzel, "Boosting Green GaInN/GaN Light-Emitting Diode Performance by a GaInN Underlying Layer," *IEEE*

Trans. Electron Devices, vol. 57, no. 10, pp. 2639–2643, Oct. 2010, doi: 10.1109/TED.2010.2061233.

[7] T.-P. Lu *et al.*, "The advantage of blue InGaN multiple quantum wells light-emitting diodes with p-AlInN electron blocking layer," *Chinese Phys. B*, vol. 20, no. 9, p. 098503, Sep. 2011, doi: 10.1088/1674-1056/20/9/098503.

[8] D. Saguatti *et al.*, "Investigation of efficiency-droop mechanisms in multi-quantum-well InGaN/GaN blue light-emitting diodes," *IEEE Trans. Electron Devices*, vol. 59, no. 5, pp. 1402–1409, May 2012, doi: 10.1109/TED.2012.2186579.

[9] M. A. Menokey, D. Nirmal, P. Prajoon, and J. C. Pravin, "Green InGaN/GaN LEDs with p-GaN interlayer for efficiency droop improvement," in *Proceedings of the 3rd International Conference on Devices, Circuits and Systems, ICDCS 2016*, 2016, pp. 216–219, doi: 10.1109/ICDCSyst.2016.7570595.

[10] S. Ishimoto *et al.*, "Enhanced Device Performance of GaInN-Based Green Light-Emitting Diode with Sputtered AlN Buffer Layer," *Appl. Sci.*, vol. 9, no. 4, p. 788, Feb. 2019, doi: 10.3390/app9040788.

[11] R. Saroosh, T. Tauqeer, S. Afzal, and H. Mehmood, "Performance enhancement of AlGaN/InGaN MQW LED with GaN/InGaN superlattice structure," *IET Optoelectron.*, vol. 11, no. 4, pp. 156–162, Aug. 2017, doi: 10.1049/iet-opt.2016.0141.

[12] T. Akasaka, H. Gotoh, Y. Kobayashi, H. Nakano, and T. Makimoto, "InGaN quantum wells with small potential fluctuation grown on InGaN underlying layers," *Appl. Phys. Lett.*, vol. 89, no. 10, p. 101110, Sep. 2006, doi: 10.1063/1.2347115.

[13] Y. Takahashi *et al.*, "Enhanced radiative efficiency in blue (In,Ga)N multiple-quantum-well light-emitting diodes with an electron reservoir layer," *Phys. E Low-dimensional Syst. Nanostructures*, vol. 21, no. 2–4, pp. 876–880, Mar. 2004, doi: 10.1016/J.PHYSE.2003.11.142.

[14] N. Nanhui *et al.*, "Enhanced luminescence of InGaN/GaN multiple quantum wells by strain reduction," *Solid. State. Electron.*, vol. 51, no. 6, pp. 860–864, Jun. 2007, doi: 10.1016/J.SSE.2007.04.007.

[15] S. Kusanagi, Y. Kanitani, Y. Kudo, K. Tasai, A. A. Yamaguchi, and S. Tomiya, "InGaN quantum wells with improved photoluminescence properties through strain-controlled modification of the InGaN underlayer," *Jpn. J. Appl. Phys.*, vol. 58, no. SC, 2019, doi: 10.7567/1347-4065/ab0f11.

[16] J. W. Ju *et al.*, "Metal-organic chemical vapor deposition growth of InGaN/GaN high power green light emitting diode: Effects of InGaN well protection and electron reservoir layer," *J. Appl. Phys.*, vol. 102, no. 5, 2007, doi: 10.1063/1.2776218.

[17] P. T. Törmä *et al.*, "Effect of InGaN underneath layer on MOVPE-grown InGaN/GaN blue LEDs," *J. Cryst. Growth*, vol. 310, no. 23, pp. 5162–5165, Nov. 2008, doi: 10.1016/j.jcrysgro.2008.07.031.

[18] N. Nanhui *et al.*, "Improved quality of InGaN/GaN multiple quantum wells by a strain relief layer," *J. Cryst. Growth*, vol. 286, no. 2, pp. 209–212, Jan. 2006, doi:

10.1016/j.jcrysgro.2005.09.027.

[19] A. M. Armstrong, B. N. Bryant, M. H. Crawford, D. D. Koleske, S. R. Lee, and J. J. Wierer, "Defect-reduction mechanism for improving radiative efficiency in InGaN/GaN light-emitting diodes using InGaN underlayers," *J. Appl. Phys.*, vol. 117, no. 13, Apr. 2015, doi: 10.1063/1.4916727.

[20] D.-P. Han *et al.*, "Role of surface defects in the efficiency degradation of GaInN-based green LEDs," *Appl. Phys. Express*, vol. 13, no. 1, p. 012007, Dec. 2020, doi: 10.7567/1882-0786/AB5BF7.

[21] A. Alkauskas, C. E. Dreyer, J. L. Lyons, and C. G. Van de Walle, "Role of excited states in Shockley-Read-Hall recombination in wide-band-gap semiconductors," May 2016, doi: 10.1103/PhysRevB.93.201304.

[22] A. Y. Polyakov *et al.*, "Effects of InAlN underlayer on deep traps detected in near-UV InGaN/GaN single quantum well light-emitting diodes," *J. Appl. Phys.*, vol. 126, no. 12, Sep. 2019, doi: 10.1063/1.5122314.

[23] M. Auf der Maur, B. Galler, I. Pietzonka, M. Strassburg, H. Lugauer, and A. Di Carlo, "Trap-assisted tunneling in InGaN/GaN single-quantum-well light-emitting diodes," *Appl. Phys. Lett.*, vol. 105, no. 13, p. 133504, Sep. 2014, doi: 10.1063/1.4896970.

[24] M. Mandurrino *et al.*, "Physics-based modeling and experimental implications of trap-assisted tunneling in InGaN/GaN light-emitting diodes," *Phys. Status Solidi Appl. Mater. Sci.*, vol. 212, no. 5, pp. 947–953, May 2015, doi: 10.1002/pssa.201431743.

[25] R. Pässler, "Photoionization cross-section analysis for a deep trap contributing to current collapse in GaN field-effect transistors," *J. Appl. Phys.*, vol. 96, no. 1, pp. 715–722, 2004, doi: 10.1063/1.1753076.

[26] A. Armstrong, T. A. Henry, D. D. Koleske, M. H. Crawford, and S. R. Lee, "Quantitative and depth-resolved deep level defect distributions in InGaN/GaN light emitting diodes," *Opt. Express*, vol. 20, no. S6, p. A812, Nov. 2012, doi: 10.1364/oe.20.00a812.

[27] K. Muraki, S. Fukatsu, Y. Shiraki, and R. Ito, "Surface segregation of in atoms during molecular beam epitaxy and its influence on the energy levels in InGaAs/GaAs quantum wells," *Appl. Phys. Lett.*, vol. 61, no. 5, pp. 557–559, 1992, doi: 10.1063/1.107835.

[28] C. Haller *et al.*, "GaN surface as the source of non-radiative defects in InGaN/GaN quantum wells," *Appl. Phys. Lett.*, vol. 113, no. 11, Sep. 2018, doi: 10.1063/1.5048010.

[29] A. David, N. G. Young, C. A. Hurni, and M. D. Craven, "Quantum Efficiency of III-Nitride Emitters: Evidence for Defect-Assisted Nonradiative Recombination and its Effect on the Green Gap," *Phys. Rev. Appl.*, vol. 11, no. 3, p. 031001, Mar. 2019, doi: 10.1103/PhysRevApplied.11.031001.